AAS 23-227

SYNODIC RESONANT HALO ORBITS IN THE HILL RESTRICTED FOUR-BODY PROBLEM

Rohith Reddy Sanaga* **and Kathleen C. Howell†**

Models representing four-body problems (4BPs) offer useful dynamical environments to investigate the impact of the Sun on behavior near the Earth-Moon libration points. Four-body models include the Bicircular Restricted Four-Body Problem (BCR4BP) and the Quasi-Bicircular Four-Body Problem (QBC4BP). The BCR4BP is widely used to examine the dynamics in the region that includes the synodic resonant near-rectilinear halo orbits (NRHO). This analysis is focused on the utility of the Hill Restricted Four-Body problem (HR4BP), a coherent four-body model, in further investigation of the dynamics in the vicinity of the Earth-Moon L_2 halo orbits. The Reduced-Hill Restricted Four-Body problem (RHR4BP), a simplified version of the HR4BP, is introduced and applied to investigate the dynamics in a particularly sensitive region along the Earth-Moon L_2 halo orbit family.

INTRODUCTION

A significant goal for NASA's current efforts in the Earth-Moon system focuses on establishment of a sustainable presence in the vicinity and on the surface of the Moon.[1] The Gateway facility is proposed as a cislunar outpost to advance the return of humans to the surface of the Moon[2] and to ultimately drive exploration and science activity further into deep space. The current baseline orbit for the Gateway is a Near Rectilinear Halo Orbit (NRHO) in the vicinity of the Moon.[3] Therefore, it is essential to examine the underlying dynamical structures in this region namely, the Earth-Moon L_2 region. Although the Earth-Moon Circular Restricted Three-Body Problem (CR3BP) provides a good approximation for the dynamics in this region, incorporating solar gravity and accommodating the pulsation of the Earth-Moon orbit supplies additional insight into behaviors in this region of cislunar space.

Models reflecting a four-body problem (4BP) include solar gravity and serve as intermediate models between the CR3BP and the Higher-Fidelity Ephemeris Model (HFEM). Some examples of the 4BPs include the Bicircular Restricted Four-Body Problem (BCR4BP) and the Quasi-Bicircular Four Body problem (QB4BP). The BCR4BP is a time-periodic model that assumes circular motions for the Earth, Moon, and Sun with respect to the Earth-Moon Barycenter.[4] The BCR4BP is widely employed to incorporate solar gravity into the dynamics in the cislunar region by multiple authors. Boudad et al.[5] use the BCR4BP to explore disposal trajectories in the NRHO region, Scheuerle et al.[6] investigate Ballistic Lunar Trajectories (BLT) in this space and Mccarthy et al.[7] explore the application of quasi-periodic orbits to BLTs using the BCR4BP. The BCR4BP also aids in overcoming

*Ph.D. Student, School of Aeronautics and Astronautics, Purdue University, West Lafayette, IN 47907; rsanaga@purdue.edu

†Hsu Lo Distinguished Professor, School of Aeronautics and Astronautics, Purdue University, West Lafayette, IN 47907; howell@purdue.edu

some of the challenges in a direct transition process of the trajectory to higher-fidelity models. Davis et al.[8] demonstrate that the particular trajectories in the Earth-Moon L_2 halo region in the vicinity of 3:1 resonant orbits present notable numerical challenges when being directly transitioned to a full ephemeris model. Although the dynamical origins of the numerical sensitivities are not clear, Boudad et al.[9] illustrate that the BCR4BP aids in overcoming some of these numerical limitations. The Quasi-Bicircular 4BP is a restricted 4BP where three major masses are revolving in a quasi-bicircular motion,[10] and with a fourth mass being small and not influencing the motion of the three primaries. Previous analyses of the dynamics in the vicinity of the Earth-Moon L_2 point leverage this model.[11,12]

The BCR4BP and the QB4BP do possess some limitations, however.[13] The BCR4BP is a non-coherent model since the primaries are assumed to be moving on circular orbits. The QB4BP is a coherent model but the analysis of the dynamics poses challenges because of the increased complexity. As an alternative, this investigation assesses the viability of the Hill Restricted Four-Body Problem (HR4BP)[14,15] in examining the dynamics in the Earth-Moon L_2 region, particularly in the sensitive 3:1 resonant region. The HR4BP is a coherent 4BP model that includes the Sun's gravity and the Earth-Moon distance pulsation. This analysis develops a simplified version of the HR4BP, namely, the Reduced-Hill Restricted Four-Body problem (RHR4BP), to investigate the dynamics in the Earth-Moon L_2 region. The RHR4BP is constructed by removing the direct perturbation of the Sun on the spacecraft, from the Sun-Earth-Moon HR4BP. The RHR4BP can be viewed as complementary to the BCR4BP because it accommodates the Sun's perturbation on the Earth-Moon motion. On the contrary, the Sun-Earth-Moon BCR4BP incorporates the direct perturbation of the Sun on the spacecraft. The HR4BP and RHR4BP model the Earth-Moon motion as the "variation orbit". The variation orbit was first introduced by G.W.Hill as a first-order approximation to the motion of the Moon in his lunar theory.[16,17] Furthermore, the variation orbit was also employed to derive first-order approximations for the lunar inequalities[18] belonging to Euler's five classes.[19] Olikara et al.[20] also apply the HR4BP to investigate planar dynamical structures in the vicinity of the Earth-Moon collinear libration point regions. It is observed that the HR4BP offers a dynamical equivalent to the L_2 point which is not observed in the BCR4BP region, suggesting that the BCR4BP has some limitations in analysing the dynamics in the vicinity of L_2 region. Therefore, it is of interest to employ the variation orbit as a lower-fidelity model for the relative motion of the Earth-Moon. This current analysis offers frameworks to construct periodic orbits in the RHR4BP, more specifically, synodic resonant orbits in the Earth-Moon L_2 region. The results are investigated to gather further insight into the dynamics in the uniquely sensitive region near the 3:1 resonant L_2 halo orbit and to compare the effects of the Sun and the Earth-Moon pulsation in this region. Davis et.al[8] present the numerical challenges in transitioning the solutions from the "transition region", defined as the region containing the Earth-Moon L_2 southern halo orbits with perilune radius in the range (10000 km, 22000 km). The characteristics noted by Davis et al.[8] are for their specific results but subsequent work indicates that the region is not rigidly defined, and work continues on better understanding of this region. The goal of the current effort is focused on the applicability of the RHR4BP (and HR4BP) in the Earth-Moon libration point regions.

BACKGROUND

Three dynamical models are employed in this investigation. The first model is the familiar Circular-Restricted Three Body Problem (CR3BP) that is extensively used to model the dynamics in cislunar space. The second model is the HR4BP, a coherent model, to represent the Sun-Earth-Moon

dynamics. Finally, the RHR4BP model is derived from the HR4BP.

The Circular Restricted Three Body Problem (CR3BP)

The CR3BP is a simplified model that models the dynamics of three bodies (M_1, M_2, M_3) that move under the influence of their mutual gravitational forces.[21] The following assumptions reduce the general three-body problem to the CR3BP: (i) The mass M_3 is negligible compared to the other masses (M_1, M_2); (ii) The other masses (called the primaries) move in a circular orbit about their mutual Barycenter (B_1). The equations of motion for the third body (M_3) are formulated in a rotating frame with an angular velocity corresponding to the circular orbit of the primaries. A rotating frame is defined with unit vectors $\hat{x}, \hat{y}, \hat{z}$ such that $\hat{x}$-axis is always directed from M_1 to M_2, $\hat{z}$ is parallel to the angular momentum vector for the orbit of M_1, M_2 and $\hat{y} = \hat{z} \times \hat{x}$. Additionally, the dynamical quantities (mass, position, and time) are non-dimensionalized such that the characteristic quantities are defined as: (i) $m^* = M_1 + M_2$; (ii) $l^* =$ radius of the circular orbit; (iii) $t^* = \sqrt{\frac{(l^*)^3}{Gm^*}}$, where G is the gravitational constant. The non-dimensional equations of motion of M_3 are then expressed as:

$$\ddot{x} = 2\dot{y} + \frac{\partial U^*}{\partial x}, \quad \ddot{y} = -2\dot{x} + \frac{\partial U^*}{\partial y}, \quad \ddot{z} = \frac{\partial U^*}{\partial z} \tag{1}$$

where U^*, the psuedo-potential function, is defined as:

$$U^* = \frac{1}{2}(x^2 + y^2) + \frac{1-\nu}{\sqrt{(x+\nu)^2 + y^2 + z^2}} + \frac{\nu}{\sqrt{(x-1+\nu)^2 + y^2 + z^2}} \tag{2}$$

Then, x, y, z are the non-dimensional coordinates of M_3 and $\nu = \frac{M_2}{M_1+M_2}$ is the non-dimensional mass of M_2. To model the dynamics of a spacecraft in the Earth-Moon CR3BP system, M_3 represents the spacecraft and M_1, M_2 are Earth and Moon, respectively.

The Hill Restricted Four-Body Problem (HR4BP)

As an alternative approach to model the behavior of four bodies, the HR4BP is a simplified four-body problem model as detailed by Scheeres.[14] The motion of an infinitesimal mass (M_3) under the gravitational influence of any two primaries (M_1, M_2) orbiting a larger mass (M_0) is represented. The following assumptions define the HR4BP: (i) The mass M_0 dominates the system ($M_0 >> M_1, M_2, M_3$); (ii) The bodies M_1, M_2 and M_3 are nearby to each other (in position space); (iii) The center of mass of M_1, M_2, M_3 is a finite distance from the body M_0; (iv) The mass M_3 is infinitesimal compared to the other masses ($M_3 << M_1, M_2$). Under these assumptions, the HR4BP is a coherent model and the relative motion of M_1, M_2 occurs in the same plane as M_0 such that the motion of M_0, M_1, M_2 is governed by the Hill Restricted three body problem (HR3BP) equations of motion.[16] Similar to the CR3BP, the HR3BP equations are non-integrable. However, a few particular solutions are available. The HR4BP leverages the variation orbit family to model the relative motion of M_1, M_2. The solution is expressed as a Fourier series with a parameter m where $2\pi m$ is the period (non-dimensional) of a family member.[14,22]

The equations of motion for M_3 are then formulated in a coordinate system rotating with an angular velocity equal to $(1 + 1/m)$ and perpendicular to the plane of M_0, M_1, M_2. This frame is referenced as the $M_1 - M_2$ rotating frame. For the Sun-Earth-Moon system, the $M_1 - M_2$ rotating frame defines the Earth-Moon (E-M) rotating frame. The origin is located at the $M_1 - M_2$ barycenter

(B_1). A constant mass, length, and time scaling is selected to derive the HR4BP equations of motion and are deduced as follows:[14]

$$\ddot{x} = 2(1+m)\dot{y} + \frac{\partial V}{\partial x}, \quad \ddot{y} = -2(1+m)\dot{x} + \frac{\partial V}{\partial y}, \quad \ddot{z} = \frac{\partial V}{\partial z} \tag{3}$$

where

$$\begin{aligned} V(x,y,z,\tau;\nu,m) = {} & \frac{1}{2}\left(1+2m+\frac{3}{2}m^2\right)(x^2+y^2) - \frac{1}{2}m^2z^2 \\ & + \frac{3}{4}m^2((x^2-y^2)\cos 2\tau - 2xy\sin 2\tau) + \frac{m^2}{a_0^3}\left[\frac{1-\nu}{R_{1-\nu}} + \frac{\nu}{R_\nu}\right] \end{aligned} \tag{4}$$

$$R_{1-\nu} = \sqrt{[x+\nu(1+\bar{\xi})]^2 + [y+\nu\bar{\eta}]^2 + z^2} \tag{5}$$

$$R_\nu = \sqrt{[x-(1-\nu)(1+\bar{\xi})]^2 + [y-(1-\nu)\bar{\eta}]^2 + z^2} \tag{6}$$

$$\bar{\xi}(\tau;m) = \sum_{n=1}^{\infty}\left(\frac{a_n(m)}{a_0(m)} + \frac{a_{-n}(m)}{a_0(m)}\right)\cos 2n\tau \tag{7}$$

$$\bar{\eta}(\tau;m) = \sum_{n=1}^{\infty}\left(\frac{a_n(m)}{a_0(m)} - \frac{a_{-n}(m)}{a_0(m)}\right)\sin 2n\tau \tag{8}$$

The HR4BP equations (Eq. (3)) are time-periodic with period 2π and contain two free parameters, ν and m. For modeling the M_1, M_2 system, the parameter ν represents the non-dimensional mass of M_2. Then, the values of coefficients $a_n(m)$ are evaluated to order m^6.[14] This approximation is a good assumption when the value of m is small and is valid for the Earth-Moon system where $m \approx 0.0808$. For the Sun-Earth-Moon system, M_0 is Sun, M_1 is Earth, M_2 is the Moon and M_3 is the spacecraft. The parameters are then evaluated as:

$$\nu = \frac{M_2}{M_1+M_2} \approx 0.01215, \quad m = \frac{n'/n}{1-n'/n} \approx 0.0808 \tag{9}$$

where n' and n are the mean motions of the Sun in the Sun-B_1 (where B_1 is the Earth-Moon barycenter) system and of the Moon around the Earth. The characteristic quantities are then defined as:

$$m^* = M_0 \text{ (Mass of Sun)} \tag{10}$$

$$l^* = l_s \times a_0 \times \left(\frac{M_1+M_2+M_3}{M_0}\right)^{1/3}, \; l_s \text{ is the distance between } B_2 \text{ and } B_1 \tag{11}$$

$$t^* = m \times n' = (1+m)n \tag{12}$$

where B_2 is the barycenter for the entire system (M_0, M_1, M_2, M_3).

The Reduced-Hill Restricted Four-Body Problem (RHR4BP)

As the name suggests, the RHR4BP is a simplified version of the HR4BP. This model is produced by removing the direct perturbation of M_0 on M_3. In the Sun-Earth-Moon case, this step corresponds to neglecting the Sun's direct perturbation on the spacecraft. As a consequence, the model is incoherent. However, the Sun still influences the motion of the Earth and the Moon. Therefore,

the relative motion of the Earth and Moon is still described by the variation orbit (Eq. (7), Eq. (8)). The equations of motion governing the infinitesimal mass M_3 in the Earth-Moon rotating frame are expressed as follows:

$$\ddot{x} = 2(1+m)\dot{y} + \frac{\partial W}{\partial x}, \quad \ddot{y} = -2(1+m)\dot{x} + \frac{\partial W}{\partial y}, \quad \ddot{z} = \frac{\partial W}{\partial z} \tag{13}$$

where

$$W(x, y, z, \tau; \nu, m) = \frac{1}{2}\left(1 + 2m + m^2\right)(x^2 + y^2) + \frac{m^2}{a_0^3}\left[\frac{1-\nu}{R_{1-\nu}} + \frac{\nu}{R_\nu}\right] \tag{14}$$

Figure 1 illustrates the motion of Earth and Moon in the E-M rotating frame. The positions of Earth (x_e, y_e, z_e) and Moon (x_m, y_m, z_m) in this frame are described by:

$$(x_e, y_e, z_e) = (-\nu(1+\bar{\xi}), -\nu\eta, 0) \tag{15}$$

$$(x_m, y_m, z_m) = ((1-\nu)(1+\bar{\xi}), (1-\nu)\eta, 0) \tag{16}$$

This model serves as an intermediate model between the CR3BP and the Earth-Moon Ephemeris model. Recall that m essentially models the pulsation (i.e., eccentricity) in the Earth-Moon motion. Thus, as $m = 0$ in HR4BP and RHR4BP (Eq. (3) and Eq. (13)), the CR3BP equations of motions are recovered.

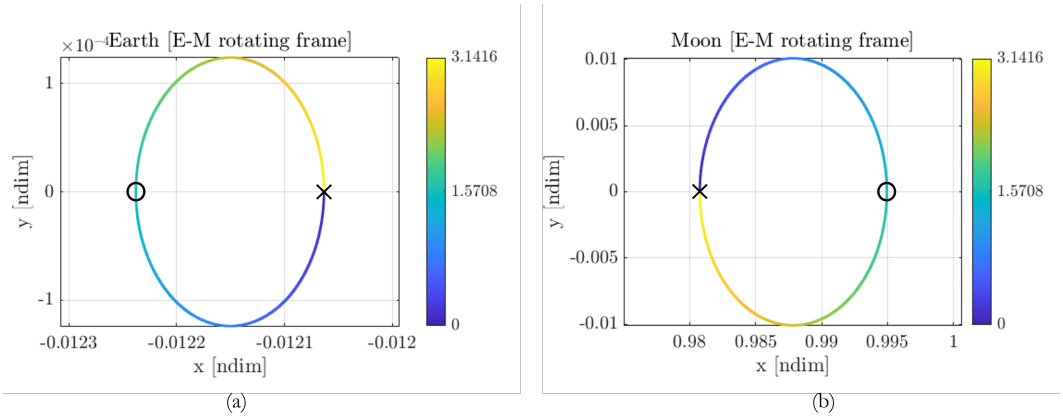

Figure 1. Motion of Earth (a) Moon (b) in RHR4BP. Colorbar represents the non-dimensional time (τ). 'x' and 'o' denotes the Earth, Moon apses at $\tau = 0$ and $\tau = \frac{\pi}{2}$ respectively.

PERIODIC ORBITS IN RHR4BP

Periodic orbits are solutions that repeat precisely in the 6D state space over every revolution. For autonomous systems, e.g., the CR3BP, it is previously demonstrated that infinitely many periodic orbits exist.[23,24] In the autonomous CR3BP, periodic orbits always exist in families. However, in non-autonomous systems, periodic orbits are mostly isolated and exist only with certain periods. These isolated periodic solutions are apparent in non-autonomous models like the ER3BP[25] and the BCR4BP.[26] The non-autonomous nature of the solutions is also consistent for the RHR4BP. It is not necessary for periodic orbits to exist in a family but, as it is commensurate with the period of the system, the period for any periodic orbit in the RHR4BP is a multiple of the Sun-Earth-Moon period, that is, approximately 29.5 days or 2π non-dimensional units.

The process for computing periodic orbits in RHR4BP is similar to the process employed in the ER3BP.[25,27] Consider the following transformations in the RHR4BP:

$$S_1 : (x, y, z, \dot{x}, \dot{y}, \dot{z}, k\pi + \tau) \rightarrow (x, -y, z, -\dot{x}, \dot{y}, -\dot{z}, k\pi - \tau) \tag{17}$$

$$S_2 : (x, y, z, \dot{x}, \dot{y}, \dot{z}, k\pi + \frac{\pi}{2} + \tau) \rightarrow (x, -y, z, -\dot{x}, \dot{y}, -\dot{z}, k\pi + \frac{\pi}{2} - \tau) \tag{18}$$

where $k = 0, 1, 2, \ldots$. The equations of motion (Eq. (13)) remain invariant under the above transformations. Given the above symmetry conditions, it is apparent that an orbit is periodic in the RHR4BP, if it possesses two perpendicular crossings with the xz plane, when the primaries are at an apse (with respect to the barycenter B_1; see Figure 1). To elaborate, for an orbit, if the initial condition $(x_1, 0, z_1, 0, \dot{y}_1, 0)$ at $\tau = 0$ or $\tau = \frac{\pi}{2}$ leads to a state $(x_2, 0, z_2, 0, \dot{y}_2, 0)$ at $\tau = n\pi$ or $\tau = n\pi + \frac{\pi}{2}$ $(n = 1, 2, 3, \ldots)$ respectively, then the orbit is periodic with period $2n\pi$. Therefore, the periodic orbits in the RHR4BP model are synodic resonant, i.e., the period is a multiple of 2π (non-dimensional units).

As mentioned previously, when $m = 0$ (Eq. (13)), the CR3BP equations of motions are recovered. Therefore, a periodic orbit in the CR3BP can be continued in the parameter m to the RHR4BP, if the continuation process leads to an orbit with a period of $2n\pi$. For example, a CR3BP orbit with a minimal period of $T_c = \frac{2q\pi}{p}$ ($\frac{p}{q}$ is a positive rational number), leads to a periodic orbit in the RHR4BP with a period equal to $2q\pi$. Then, p is the number of revolutions for the spacecraft along its orbit in the time required for the primaries to complete q revolutions. The ratio $\frac{p}{q}$ denotes the resonance ratio. In Figure 2, the Earth-Moon southern L_2 halo orbit family and the resonance ratio across the family members are plotted. The L_2 halo orbit family is a spatial family of orbits in the CR3BP that bifurcate from the planar L_2 Lyapunov orbits and evolves out-of-plane as the family approaches the Moon. These orbits are symmetric across the xy plane. The transition region, although not clearly defined, consists of the orbits near the 3:1 resonant orbit.[8]

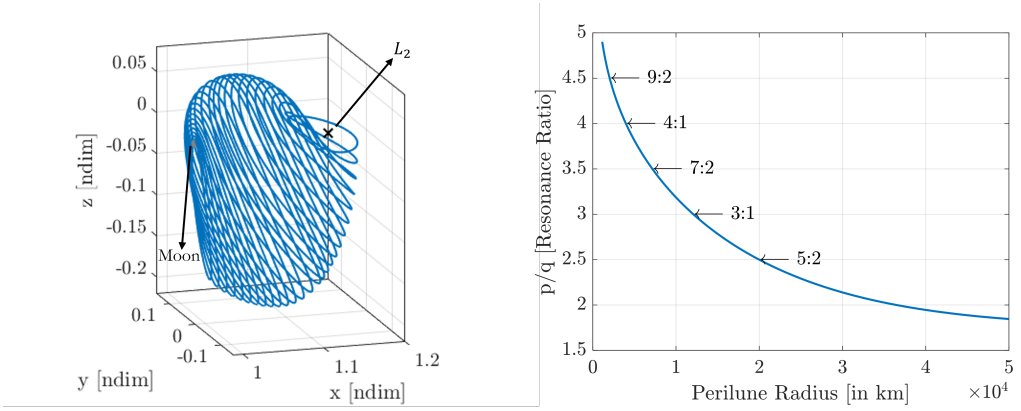

(a) (b)

Figure 2. (a) Earth-Moon L_2 southern halo orbit family (b) Resonance ratio for the family members

Perpendicular Crossing Algorithm

As Noted previously, periodic orbits in the RHR4BP are constructed by enforcing perpendicular crossings when the primaries are located at an apse. The L_2 halo family in the CR3BP is symmetric across the xz plane with two perpendicular crossings. Therefore, a continuation process in the parameter m ($m = 0$ (CR3BP) to $m \approx 0.0808$ (RHR4BP)) produces periodic orbits in the RHR4BP. Additionally, for a $p : q$ resonant orbit in the CR3BP, two RHR4BP counterparts exist corresponding to the two symmetry conditions (Eqs. (17), (18)). The two counterparts are denoted by A and B. The 3:1 L_2 halo counterparts are illustrated in Figures 3 and 4. Note that the 3:1 sidereal resonant orbit in CR3BP is leveraged for the continuation procedure. However, the counterpart produced in the RHR4BP at $m \approx 0.0808$ remains synodic resonant because the non-dimensional time, includes the parameter m (Eq. (12)) in its evaluation. Therefore, a sidereal resonant orbit from CR3BP is continued to a synodic resonant orbit in the RHR4BP.

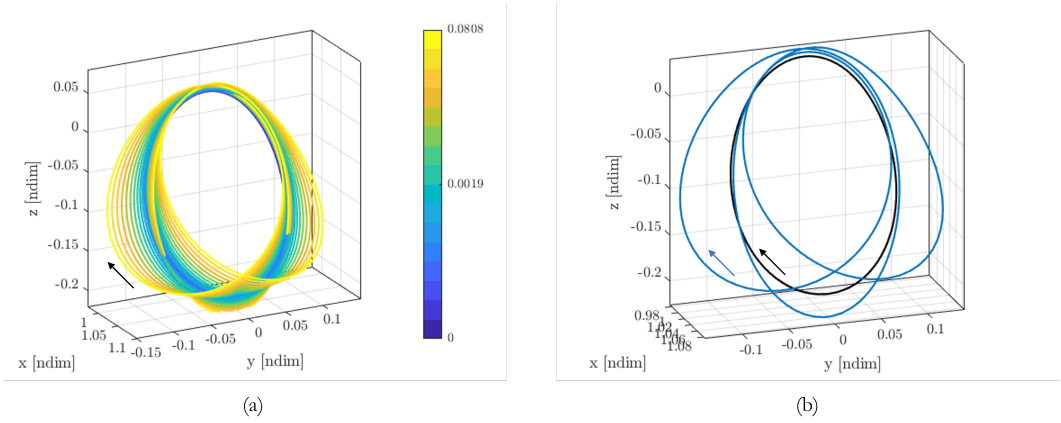

Figure 3. (a) continuation in parameter m. Colorbar denotes the variation in m (b) 3:1 Synodic Resonant L_2 Halo RHR4BP counterpart A (blue), 3:1 Sidereal Resonant Orbit in CR3BP (black)

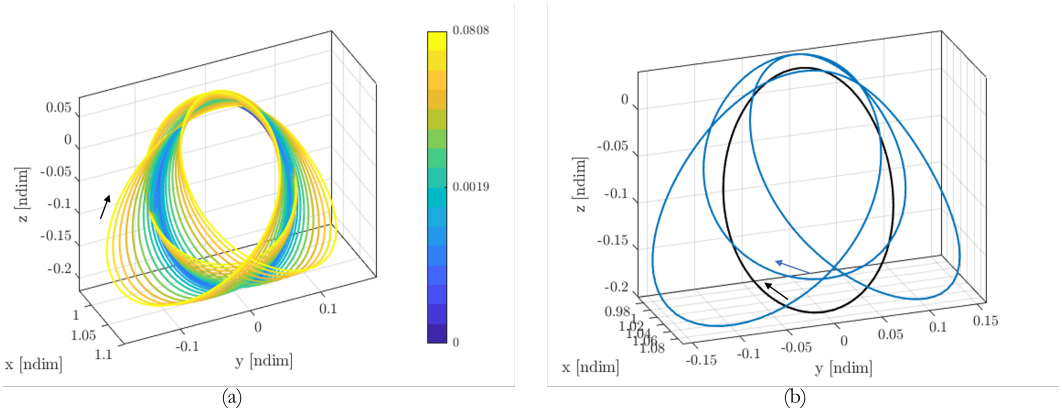

Figure 4. (a) continuation in parameter m. Colorbar denotes the variation in m (b) 3:1 Synodic Resonant L_2 Halo RHR4BP counterpart B (blue), 3:1 Sidereal Resonant Orbit in CR3BP (black)

Although the initial focus is the 3:1 resonant orbit, the construction process is not limited to a

specific resonance. An alternative example appears in Figure 5. The 4:1 synodic resonant counterparts in the RHR4BP is produced by incorporating a continuation procedure from the 4:1 sidereal resonant orbit from the CR3BP. It is noted that the geometries for the 3:1 (Counterpart A) and 4:1

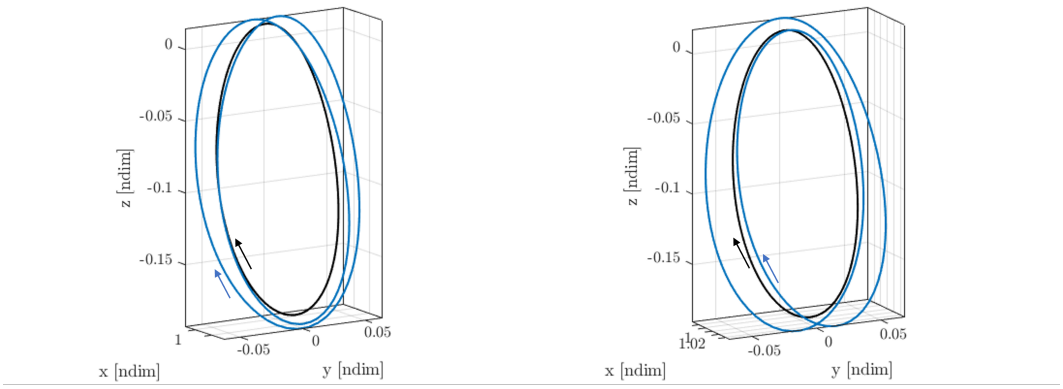

Figure 5. 4:1 synodic resonant Orbit (a) Counterpart A (blue). (b) Counterpart B (blue); 4:1 sidereal resonant Orbit in CR3BP (black)

(Counterparts A,B) are also observed in the BCR4BP.[26] However, the geometry of 3:1 counterpart B has not been knowingly observed in the BCR4BP previously. Such is an indication that the pulsation in the E-M motion (modeled in the RHR4BP) offers significant influence as compared to the direct perturbation from the solar gravity (modeled in the BCR4BP) in the transition region.

LINEAR STABILITY PROPERTIES

The stability properties for the periodic solutions in the RHR4BP are investigated for further insight into the dynamics. The eigenvalues of the monodromy matrix are employed to construct a metric for the linear stability properties. The eigenvalues of the monodromy matrix occur in pairs since the RHR4BP is a Hamiltonian system. The stability metric, i.e., the "Lyapunov exponent", associated with the monodromy matrix, is employed here. The Lyapunov exponent is selected following Boudad et.al[26] to investigate the stability of the synodic resonant periodic orbits in the BCR4BP. Therefore, it serves as a good comparison metric for the two models. The Lyapunov exponent, l_i, is defined as,

$$l_i = Real\left(\frac{\log \lambda_i}{T}\right) \tag{19}$$

where T is the orbital period and λ_i is the i^{th} eigenvalue from the monodromy matrix. Then, $l_i > 0$ corresponds to an expansion when a perturbation is introduced in the 6D phase space of the orbit. Correspondingly, $l_i < 0$ identifies a contraction. Finally, $l_i = 0$ when the eigenvalue is on the unit circle. This case corresponds to an absence of divergence when a perturbation is introduced. Therefore, the sign of the Lyapunov exponent determines the stability of a periodic solution in the linear sense. Thus, the necessary condition for linear stability is that all the Lyapunov exponents are zero.[21,26] Since a constant of integration (Jacobi Constant) exists in the CR3BP and as a Hamiltonian system, there exists a unit pair of eigenvalues for every periodic orbit. Such behaviour is absent in the RHR4BP.

Consider the 3:1 resonant families (with parameter m) as displayed in Figures 3 and 4. The Lyapunov exponents for orbits in the families are plotted in Figure 6. In Figure 6 (a), for, the family corresponding to counterpart A, the parameter m appears as function of the Lyapunov exponents. At $m = 0$, that corresponds to the 3:1 sidereal orbit in CR3BP, there are 4 eigenvalues on the unit circle. Upon continuation, the two trivial eigenvalues move along the unit circle. Additionally, for the counterpart B family (Figure 4), as m evolves, the two trivial eigenvalues move along the real axis such that the two lines split from the $l_i = 0$ line. A distinguishing feature of these plots is that the continuation process that evolves with m, is marked with many bifurcations. Further investigation of the eigenvalues reveal that the counterpart A (Figure 6 (a)) incurs two period-doubling bifurcations and two secondary-hopf bifurcations. A similar behaviour appears along the continuation evolution for counterpart B (Figure 6 (b)) as well. There is one period-doubling bifurcation and multiple secondary-hopf bifurcations.

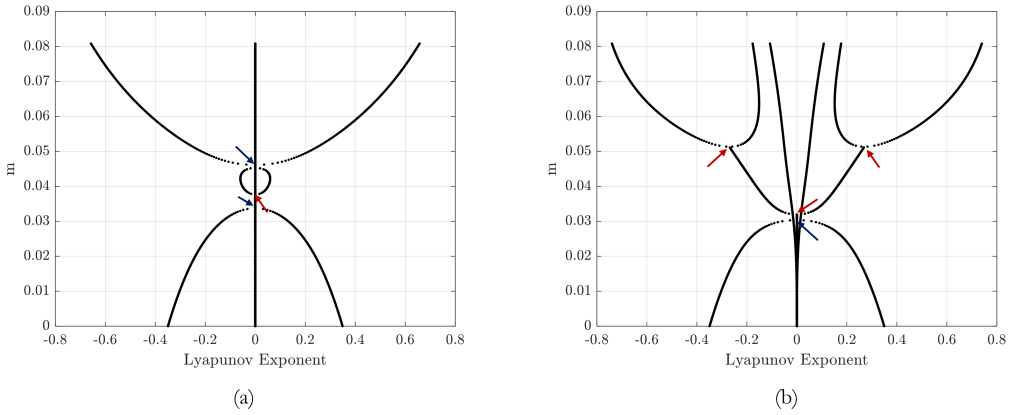

Figure 6. Lyapunov Exponents along the 3:1 synodic resonant family (a) Counterpart A (b) Counterpart B; $m = 0$ corresponds to CR3BP and $m \approx 0.0808$ corresponds to the Earth-Moon RHR4BP; red arrows point to secondary-hopf bifurcations and blue arrows point to the period-doubling bifurcations

Multiple periodic orbits near the 3:1 Synodic Resonant orbit are generated and the Lyapunov exponent behaviour is investigated to verify if stability evolution is a characteristic feature of the transition region. Figures 7 and 8 illustrate the 14:5 and 16:5 synodic resonant L_2 halo orbits and their stability properties, respectively. Both figures display bifurcation behavior similar to the 3:1 case. Upon deeper examination of the eigenvalues along the family, it is apparent that there are multiple secondary-hopf bifurcations and a tangent bifurcation in the 14:5 family (Figure 7 (b)), whereas the 16:5 family (Figure 8 (b)) yields two tangent bifurcations.

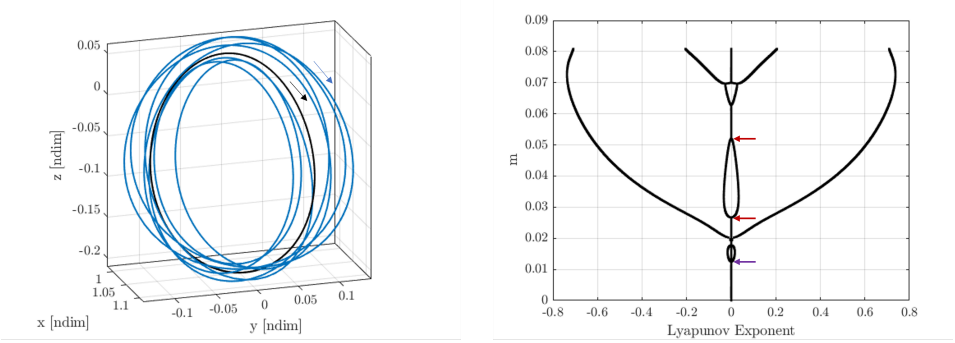

Figure 7. (a) 14:5 synodic resonant RH4BP orbit (blue) and the 14:5 sidereal resonant orbit in CR3BP (black) (b) Lyapunpov exponents along the family; $m = 0$ corresponds to CR3BP and $m \approx 0.0808$ corresponds to the Earth-Moon RHR4BP; red arrows point to some of the secondary-hopf bifurcations and purple arrow points to the tangent bifurcation

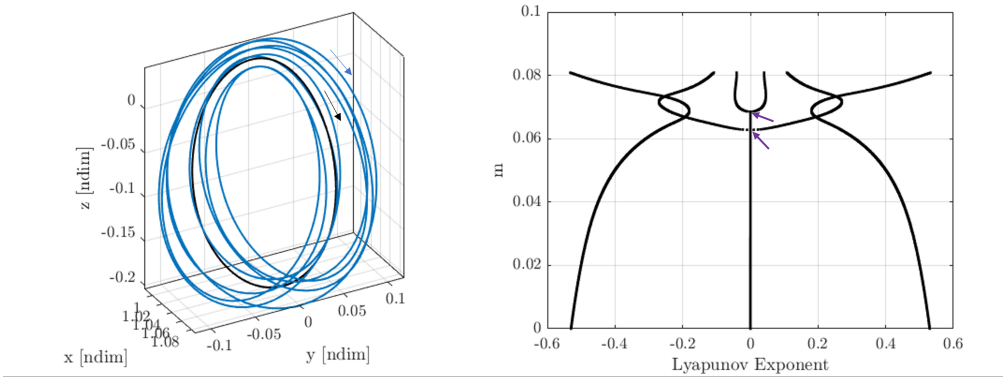

Figure 8. (a) 16:5 Synodic Resonant RH4BP orbit (blue) 16:5 Sidereal Resonant Orbit in CR3BP (black) (b) Lyapunpov Exponents along the family; $m = 0$ corresponds to CR3BP and $m \approx 0.0808$ corresponds to the Earth-Moon RHR4BP; purple arrows point to the tangent bifurcations

Figure 9 presents the lyapunov exponent behaviour for the 8:3 and 10:3 Synodic Resonant orbit families which are further away from the 3:1 orbit. As can be observed from the figures, the bifurcation behavior is less complex. Only one secondary-hopf bifurcation occurs in the families. Figure 10 shows the lyapunov exponents for the 5:2 and 11:3 synodic resonant families. There are no bifurcations in these families.

The linear stability analysis in the RHR4BP provides some insight into the specific characteristics of the transition region and also gives additional information which can be used to accurately determine the bounds of the transition region. The farther you move away from the 3:1 orbit, the bifurcation behavior is less complex with no bifurcations for the 5:2 and 11:3 families (Figure 10). Therefore, the transition region can be defined to exist between the 5:2 sidereal resonant orbit and the 11:3 sidereal resonant orbit in the CR3BP. Also, from the earlier figures, and perhaps not surprisingly, it is inferred that the stability properties of the RH4BP counterparts are different from

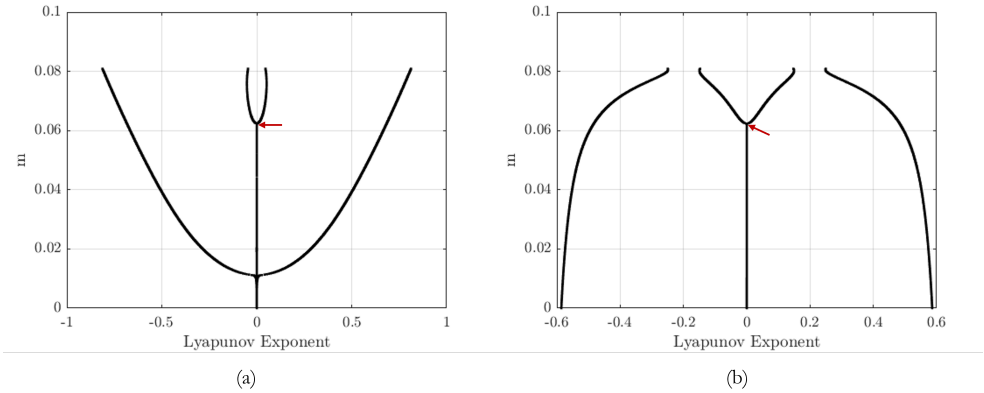

Figure 9. Lyapunpov Exponents along the family A for (a) 8:3 Synodic Resonant RH4BP orbit family (b) 10:3 Synodic Resonant RH4BP orbit family; $m = 0$ corresponds to CR3BP and $m \approx 0.0808$ corresponds to the Earth-Moon RHR4BP; red arrow points to the secondary-hopf bifurcation

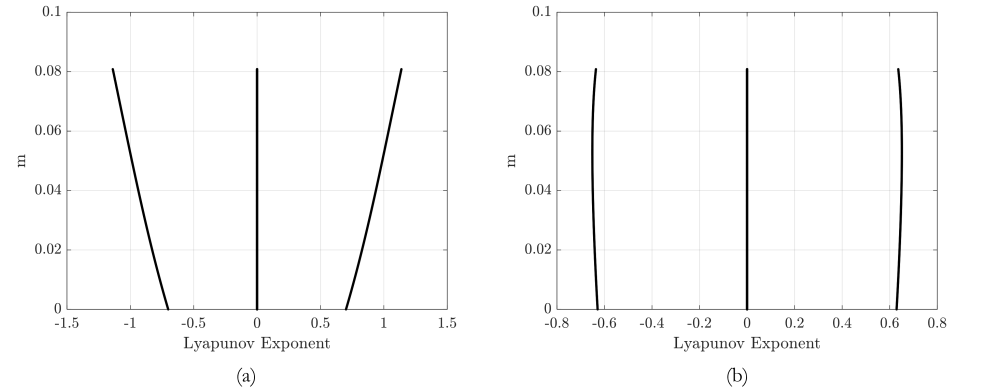

Figure 10. Lyapunpov Exponents along the family A for (a) 5:2 Synodic Resonant RH4BP orbit family (b) 11:3 Synodic Resonant RH4BP orbit family; $m = 0$ corresponds to CR3BP and $m \approx 0.0808$ corresponds to the Earth-Moon RHR4BP

their CR3BP counterparts. Furthermore, comparing the stability properties of the 3:1 family in BCR4BP[26] with the RHR4BP (Figure 6), it can be noticed that the RHR4BP gives additional insight into the dynamics. This further emphasizes that the pulsation in the Earth-Moon system is an essential component to model the dynamics in the transition region since these characteristics cannot be discerned from the CR3BP or the BCR4BP.

Period-Doubling Bifurcations in the 3:1 family

The 3:1 synodic resonant orbit and its counterparts A and B are particularly interesting as their stability evolves with increasing model fidelity. A closer look at Figure 6 is assessed in Figure 11. The period-doubling bifurcations in the families are highlighted. A period-doubling bifurcation occurs when two eigenvalues of the monodromy matrix are equal to -1. These period doubling bifurcations are further examined by generating the families that emerge from them.

Figure 12 illustrates the first period doubling bifurcation in the 3:1 family (A). A naming convention

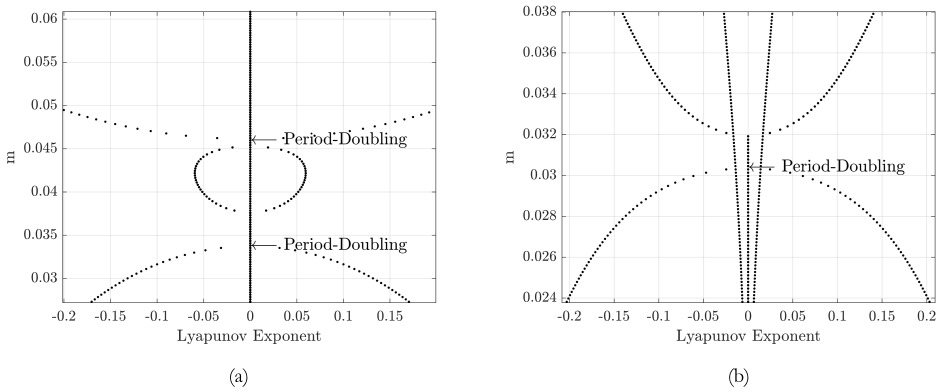

Figure 11. Zoomed version of Figure 6 identifying the period-doubling bifurcations; Lyapunov exponents along the family (a) Counterpart A (b) Counterpart B; $m = 0$ corresponds to CR3BP and $m \approx 0.0808$ corresponds to the Earth-Moon RHR4BP

for the families that evolve from the period-doubling bifurcations is defined similar to the convention introduced by Zimovan et al.[28] As an example, P2Ln corresponds to the period doubling bifurcation (P2); from the family A (L = A) and n refers to the n^{th} bifurcation. Therefore, Figure 12 reflects the P2A1 family and Figure 13 is focused on the P2A2 family. The P2A1 and P2A2 counterparts in the RHR4BP offer very different structures as compared to the 3:1 counterpart A in RHR4BP (Figure 3) and the 3:1 sidereal resonant orbit in the CR3BP. Recall that the P2A1 and P2A2 families of orbits result from the period-doubling bifurcation and possess six "lobes" whereas the 3:1 A counterpart is defined by three "lobes". Of course, the P2A1 and P2A2 are produced from the period-doubling bifurcations from the 3 "lobe", 3:1 resonant A counterpart family. The period-doubling bifurcation from the B counterpart family (Figure 11 (b)) is continued to produce the P2B1 family and is plotted in Figure 14. The P2B1 family differs from the P2A families since this family only continues "back" to the CR3BP ($m = 0$).

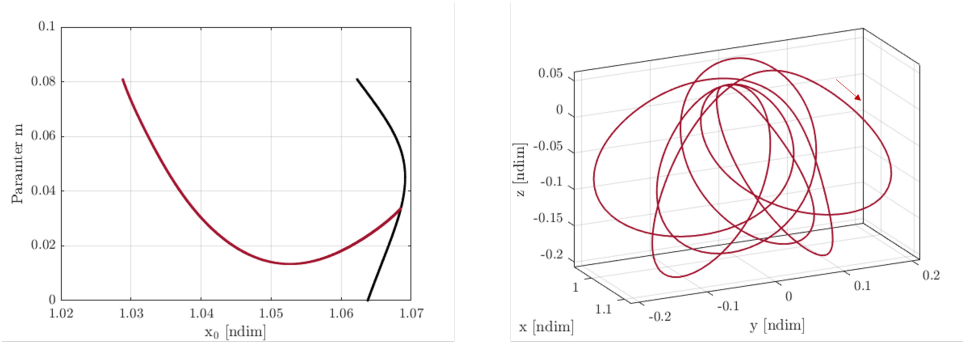

Figure 12. (a) Characteristic curve (x_0 is the initial x-location) for the 3:1 family counterpart A (black), P2A1 (red) (b) P2A1 counterpart in the Earth-Moon RHR4BP ($m \approx 0.0808$)

The L_2 halo family in the Earth-Moon CR3BP includes multiple period multiplying bifurcations and it is probable that the geometries in the RHR4BP are influenced by those structures. Since the families P2A1, P2A2 and P2B1 possess 6 lobes, the bifurcations of interest are period-doubling

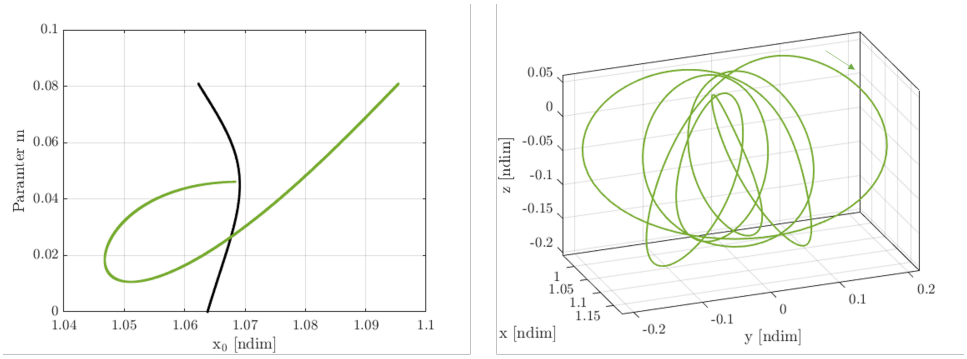

Figure 13. (a) Characteristic curve (x_0 is the initial x-location) for the 3:1 family counterpart A (black), P2A2 (green) (b) P2A2 counterpart in the Earth-Moon RHR4BP ($m \approx 0.0808$)

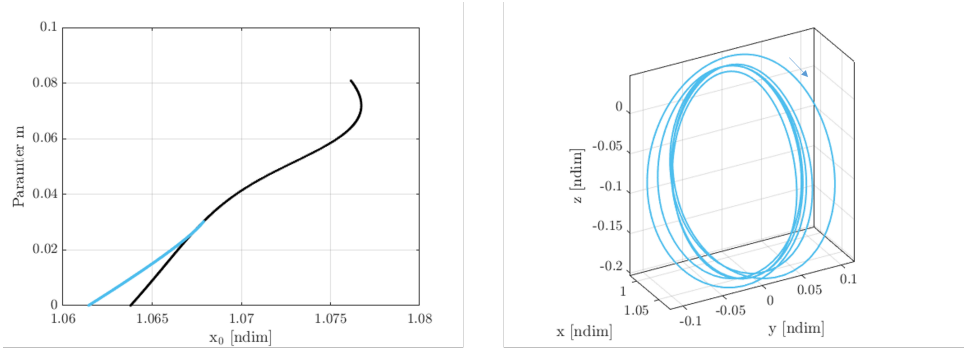

Figure 14. (a) Characteristic curve (x_0 is the initial x-location) for the 3:1 family counterpart B (black), P2B1 (blue) (b) P2B1 counterpart in the Earth-Moon CR3BP ($m = 0$)

bifurcations (P2HO), period-tripling bifurcations (P3HO) and period-six (P6HO) bifurcations. The naming convention for the orbits is as defined by Zimovan et al.[28] For example, in the 'Pn_1HOn_2' family, 'Pn_1' refers to the order of the period-multiplication (e.g., period-doubling is reflected as n_1 = 2), 'HO' refers to the family from which the bifurcating family has evolved i.e., halo family and n_2 corresponds to the sub-family identifier (for multiple bifurcations of the same type, the first family, in order of increasing perilune radius, is labeled n_2 = 1, second family is labeled as $n_2 = 2$ and so on).[28] Six lobes are produced by either three revolutions along a P2HO family member, or two revolutions of a P3HO family member or one revolution along a P6HO family member. Upon further investigation of these families, the families of interest are determined to be the P2HO2 family, P3-P2HO2 family (Period-tripling bifurcation from the P2HO2 family) and the P6HO2 family. Figure 15 (a) illustrates the P2HO2 family in the Earth-Moon CR3BP in terms of the Jacobi Constant as a function of the period. Then, in Figure 15 (b), the family member is plotted that is suitable to be continued in the parameter m to produce its counterpart in the RHR4BP with a period of 4π. This counterpart is the 3:2 P2HO2 orbit and the 3:2 synodic resonant P2HO2 family is plotted in Figure 16. The RHR4BP counterpart closely resembles the P2A1 counterpart

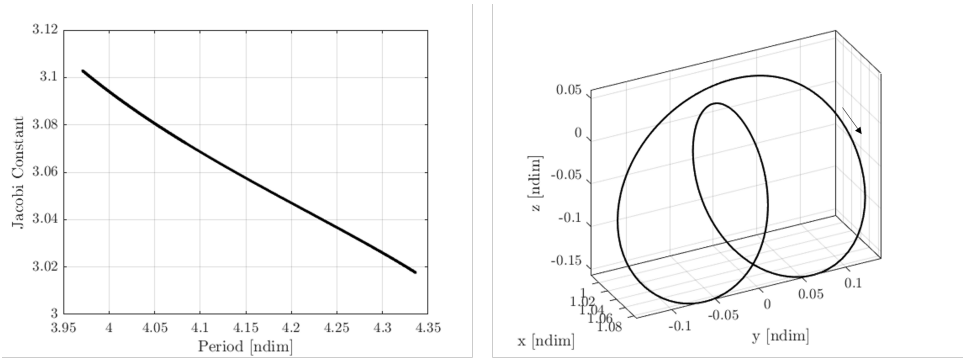

Figure 15. (a) Characteristic curve for the P2HO2 family in the Earth-Moon CR3BP (b) family member with the period $\frac{4\pi}{3}$

(Figure 12 (b)). Additionally, the 3:2 P2HO2 structure (Figure 15 (b)) potentially influences the 3-lobe geometry in the 3:1 synodic resonant Counterparts (A and B). The orbits in Figure 16 and Figure 12 are not identical, however. The P2HO2 family in the Earth-Moon CR3BP has two period-tripling bifurcations along the baseline family. However, both these bifurcations lead to the same period-tripling family, denoted by P3-P2HO2. The bifurcating orbits appear in Figure 17 along with the characteristic curve for the P2HO2 and P3-P2HO2 families. Note that the P3-P2HO2 family possesses only one family member with a period equal to 4π that can be exploited in a continuation process to produce a periodic orbit in the RHR4BP. However, the P3-P2HO2 family is interesting because the family members exhibit geometric features consistent with the P2A1 (Figure 12) and P2B1 (Figure 14) families. Figure 18 illustrates the family members from the P3-P2HO2 family that resemble the geometries for the periodic orbits in the RHR4BP. Note that the orbit in Figure 18 (c) and the orbit in Figure 14 (b) are identical, i.e., the the P2B1 orbit at $m = 0$ is a member of the P3-P2HO2 family. Although not demonstrated in this paper, the geometries from the P3-P2HO2 family also resemble the geometries in the P2A and P2B families at non-zero m values. Finally, the P6HO2 family characteristics are plotted in Figure 19; a family member is also displayed that closely resembles the geometry for the P2A2 RHR4BP counterpart (Figure 13 (b)).

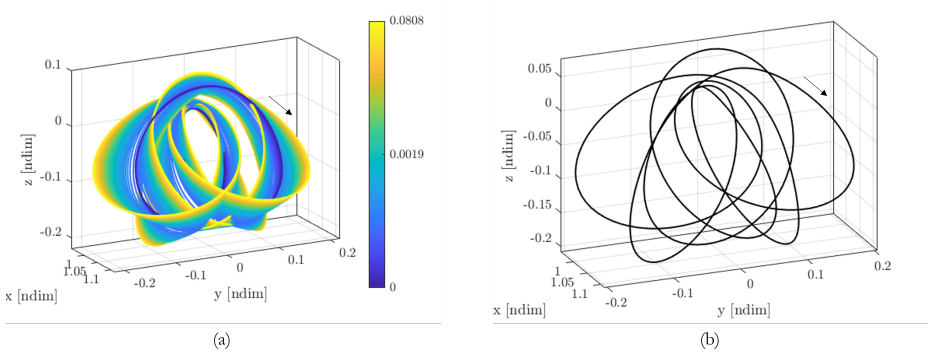

Figure 16. (a) Continuation in parameter m for the 3:2 synodic resonant P2HO2 family. Colorbar denotes the variation in m (b) 3:2 synodic resonant L_2 P2HO2 RHR4BP counterpart orbit A

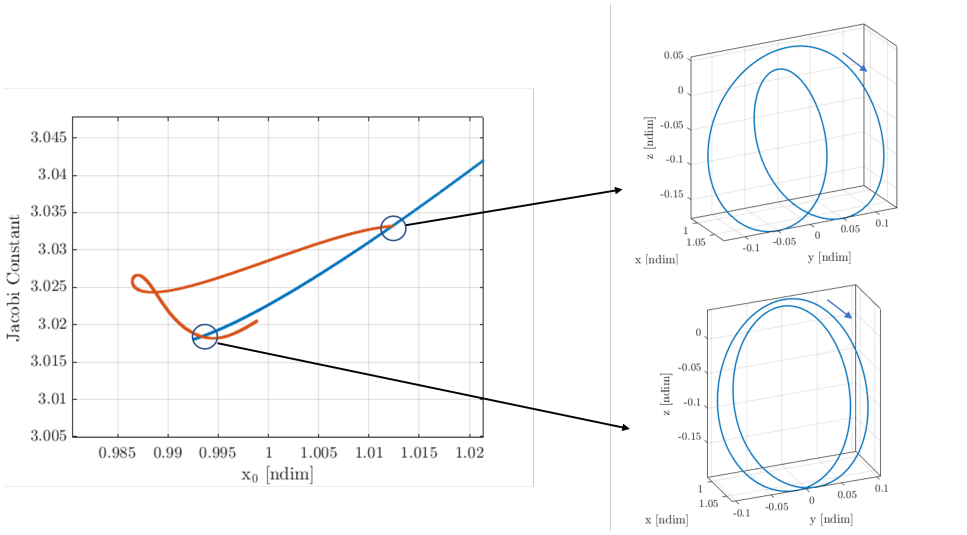

Figure 17. Period-tripling bifurcations along the P2HO2 family in the Earth-Moon CR3BP. P2HO2 family (blue); P3-P2HO2 family (orange). The bifurcating orbits lead to the same family (P3-P2HO2) and are plotted for reference

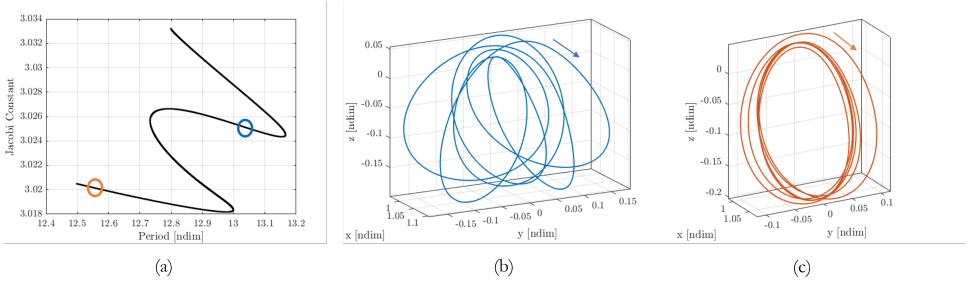

Figure 18. (a) Characteristic curve for the P3-P2HO2 family in the Earth-Moon CR3BP (b) A family member that resembles the P2A1 counterpart (c) The family member that is identical to the P2B1 counterpart in CR3BP

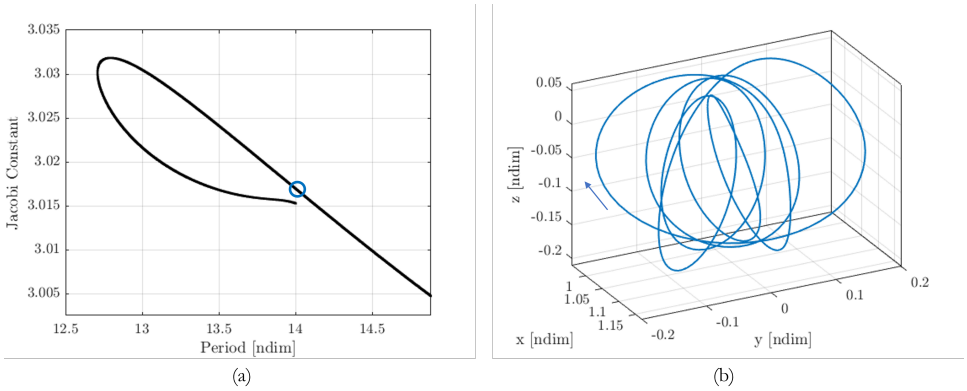

Figure 19. (a) Characteristic curve for the P6HO2 family in the Earth-Moon CR3BP (b) A family member that resembles the P2A2 counterpart

The linear stability analysis indicates that the higher-period orbit structures around the L_2 halo orbit family possibly influence the geometries in the transition region in the RHR4BP. The pulsation of the Earth-Moon motion may directly impact the dynamical environment as it is not modeled in the CR3BP model and, hence, the structures from nearby periodic families likely influence the geometries in the transition region. This complex dynamical environment likely contributes to the numerical challenges that occur when transitioning the orbits from the transition region into the ephemeris model.

IMPACT OF SOLAR GRAVITY VERSUS PULSATION

Recall that the RHR4BP is a reduced version of the HR4BP that is produced by removing the direct Sun perturbation terms from the HR4BP. Therefore, periodic solutions from the RHR4BP can be continued to the HR4BP by introducing a continuation parameter γ. Additionally, an intermediate model between the RHR4BP and the HR4BP is thus introduced as follows:

$$\ddot{x} = 2(1+m)\dot{y} + \frac{\partial \mathcal{W}}{\partial x}, \quad \ddot{y} = -2(1+m)\dot{x} + \frac{\partial \mathcal{W}}{\partial y}, \quad \ddot{z} = \frac{\partial \mathcal{W}}{\partial z} \tag{20}$$

where

$$\begin{aligned}\mathcal{W}(x,y,z,\tau;\nu,m) = \frac{1}{2}\left(1+2m+m^2\right)(x^2+y^2) + \frac{m^2}{a_0^3}\left[\frac{1-\nu}{R_{1-\nu}} + \frac{\nu}{R_\nu}\right] \\ + \gamma\left(\frac{m^2}{4}(x^2+y^2) - \frac{1}{2}m^2z^2 + \frac{3}{4}m^2((x^2-y^2)\cos 2\tau - 2xy\sin 2\tau)\right)\end{aligned} \tag{21}$$

The value for γ ranges from 0 to 1, with $\gamma = 0$ corresponding to the Sun-Earth-Moon RHR4BP and $\gamma = 1$ reflecting to the Sun-Earth-Moon HR4BP. A new parameter (ϕ), labeled the E-M phase parameter is introduced into the variation orbit as follows:

$$\bar{\xi}(\tau;m;\phi) = \sum_{n=1}^{\infty}\left(\frac{a_n(m)}{a_0(m)} + \frac{a_{-n}(m)}{a_0(m)}\right)\cos 2n(\tau+\phi) \tag{22}$$

$$\bar{\eta}(\tau;m;\phi) = \sum_{n=1}^{\infty}\left(\frac{a_n(m)}{a_0(m)} - \frac{a_{-n}(m)}{a_0(m)}\right)\sin 2n(\tau+\phi) \tag{23}$$

where ϕ adjusts the location of the Earth and the Moon in their respective orbits (Figure 1).

All the intermediate models include the same value for the parameter m. Increasing the value of γ corresponds to increasing the influence of the Sun's acting force directly on the spacecraft until $\gamma = 1$. The process to generate periodic orbits is similar to the procedure applied in the RHR4BP. A perpendicular crossing algorithm is implemented to continue the orbits from the RHR4BP along the parameter γ. However, since the Sun is now included, the phasing parameter is required to maintain the conditions for the periodic orbit from the RHR4BP. Consider the 3:1 synodic resonant orbit (counterpart A) in the RHR4BP. Since the period is 2π, the continuation process targets a perpendicular crossing at $\tau = 0, \pi$ with $\phi = \pi/2$. Similarly, for the counterpart B, the continuation process targets a perpendicular crossing at $\tau = \pi/2, 3\pi/2$ with $\phi = \pi/2$. The resulting orbit families are plotted in Figure 20 and Figure 21. Figure 22 includes the RHR4BP and HR4BP counterparts for the P2A families.

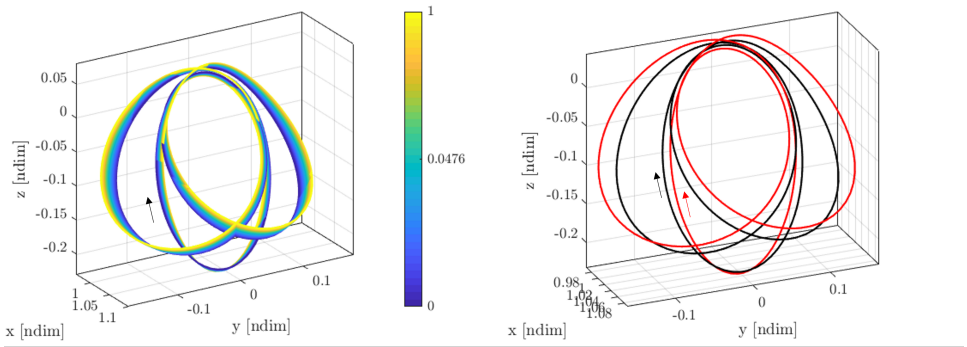

Figure 20. (a) Continuation in parameter γ for the 3:1 synodic resonant orbit (A). Colorbar denotes the variation in γ (b) 3:1 synodic resonant L_2 counterpart A in the RHR4BP (black) and HR4BP (red)

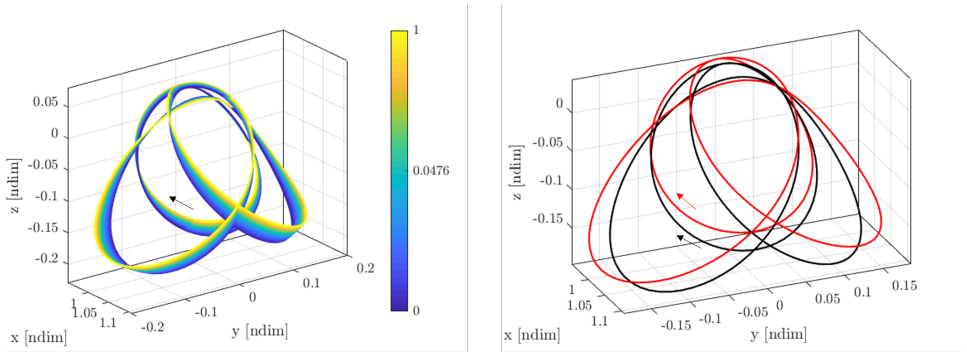

Figure 21. (a) Continuation in parameter γ for the 3:1 synodic resonant orbit (B). Colorbar denotes the variation in γ (b) 3:1 synodic resonant L_2 counterpart B in the RHR4BP (black) and HR4BP (red)

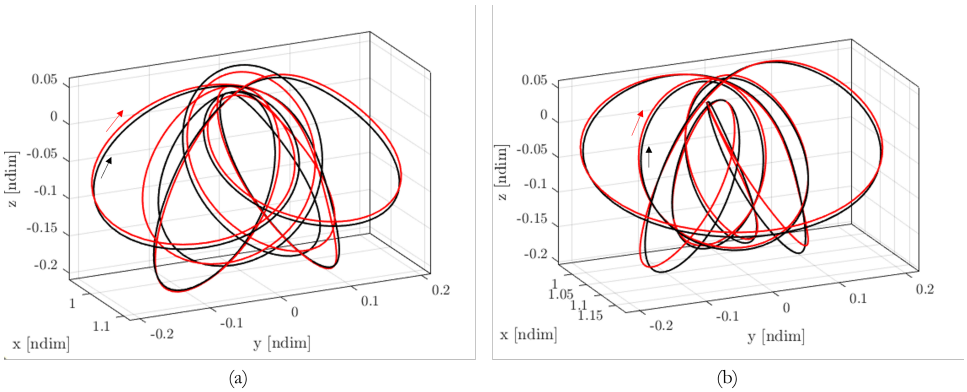

Figure 22. (a) P2A1 counterpart in the RHR4BP (black) and HR4BP (red) (b) P2A2 counterpart in RHR4BP (black) and HR4BP (red)

As apparent from the above figures, the geometries of the periodic orbits are similar in both models.

The solutions constructed in the RHR4BP persist under the addition of a direct solar perturbation. These observations support the viewpoint that the pulsation of the Earth-Moon motion is essential in capturing the true dynamics in, at least, the transition region.

CONCLUDING REMARKS

This paper includes the results from an investigation to evaluate the applicability of the HR4BP in the Earth-Moon Libration point regions. The RHR4BP, a reduced version of the HR4BP, is derived by neglecting the direct Sun perturbation on the spacecraft. Thus, the RHR4BP is a non-coherent three-body problem that incorporates the variation orbit to approximate the Earth-Moon motion. Periodic orbits are constructed in the L_2 region. As seen previously, the RHR4BP exhibits the geometries displayed in the BCR4BP and also admits additional unique solutions. Upon investigating the linear stability properties, the transition region demonstrates complex bifurcation behavior and possibly contributes to the numerical challenges faced when transitioning solutions to the ephemeris model. Furthermore, the characteristic behavior in the RHR4BP offers insight into the bounds of the transition region. Additionally, it is observed that, in the transition region, the nearby higher-period orbit structures in the L_2 halo family appear to influence the geometries in the higher-fidelity models. Moreover, the analysis completed in the RHR4BP persists in the HR4BP, suggesting that, in some regions, the pulsation of the Earth-Moon motion generates a greater influence than the direct perturbation from the solar gravity. In summary, the HR4BP is a useful addition to the CR3BP and BCR4BP models to analyze the dynamics for behaviors in the cislunar space.

REFERENCES

[1] J. C. Crusan, R. M. Smith, D. A. Craig, J. M. Caram, J. Guidi, M. Gates, J. M. Krezel, and N. B. Herrmann, "Deep space gateway concept: Extending human presence into cislunar space," *2018 IEEE Aerospace Conference*, IEEE, 2018, pp. 1–10.

[2] J. Crusan, J. Bleacher, J. Caram, D. Craig, K. Goodliff, N. Herrmann, E. Mahoney, and M. Smith, "NASA's gateway: an update on progress and plans for extending human presence to cislunar space," *2019 IEEE Aerospace Conference*, IEEE, 2019, pp. 1–19.

[3] E. M. Zimovan, K. C. Howell, and D. C. Davis, "Near rectilinear halo orbits and their application in cis-lunar space," *3rd IAA Conference on Dynamics and Control of Space Systems, Moscow, Russia*, Vol. 20, 2017, p. 40.

[4] S.-S. Huang, "Very restricted four-body problem," *Publications of Goddard Space Flight Center*, 1960, p. 354.

[5] K. K. Boudad, D. C. Davis, and K. C. Howell, "Disposal trajectories from near rectilinear halo orbits," *AAS/AIAA Astrodynamics Specialists Conference*, No. JSC-E-DAA-TN60056, 2018.

[6] S. T. Scheuerle and K. C. Howell, "Characteristics and Analysis of Families of Low-Energy Ballistic Lunar Transfers," *AAS/AIAA Astrodynamics Specialist Conference*, 2021.

[7] B. P. McCarthy and K. C. Howell, "Four-body cislunar quasi-periodic orbits and their application to ballistic lunar transfer design," *Advances in Space Research*, 2022.

[8] D. C. Davis, S. M. Phillips, K. C. Howell, S. Vutukuri, and B. P. McCarthy, "Stationkeeping and transfer trajectory design for spacecraft in cislunar space," *AAS/AIAA Astrodynamics Specialist Conference*, 2017, pp. 1–20.

[9] K. Boudad, K. C. Howell, and D. C. Davis, "Analogs for Earth-Moon Halo Orbits and their Evolving Characteristics in Higher-Fidelity Force Models," *AIAA SCITECH 2022 Forum*, 2022, p. 1276.

[10] M. Andreu, "The quasi-bicircular problem," *Ph. D. Dissertation*, 1998.

[11] M. Andreu, "Dynamics in the center manifold around L2 in the quasi-bicircular problem," *Celestial Mechanics and Dynamical Astronomy*, Vol. 84, No. 2, 2002, pp. 105–133.

[12] B. Le Bihan, J. Masdemont, G. Gómez, and S. Lizy-Destrez, "Invariant manifolds of a non-autonomous quasi-bicircular problem computed via the parameterization method," *Nonlinearity*, Vol. 30, No. 8, 2017, p. 3040.

[13] M. Jorba-Cuscó, A. Farrés, and À. Jorba, "Two periodic models for the Earth-Moon system," *Frontiers in Applied Mathematics and Statistics*, Vol. 4, 2018, p. 32.

[14] D. Scheeres, "The restricted Hill four-body problem with applications to the Earth–Moon–Sun system," *Celestial Mechanics and Dynamical Astronomy*, Vol. 70, No. 2, 1998, pp. 75–98.

[15] L. Mohn and J. Kevorkin, "Some limiting cases of the restricted four-body problem," *The Astronomical Journal*, Vol. 72, 1967, p. 959.

[16] G. W. Hill, "Researches in the lunar theory," *American journal of Mathematics*, Vol. 1, No. 1, 1878, pp. 5–26.

[17] G. W. Hill, "On the part of the motion of the lunar perigee which is a function of the mean motions of the sun and moon," *Acta mathematica*, Vol. 8, No. 1, 1886, pp. 1–36.

[18] C. Stephenson, "George Darwin's lectures on Hill's lunar theory," *Bulletin (British Society for the History of Mathematics)*, Vol. 24, No. 3, 2009, pp. 159–171.

[19] L. Euler, *Theoria motuum lunae nova methodo pertractata: una cum tabulis astronomicis*. 1772.

[20] Z. P. Olikara, G. Gómez, and J. J. Masdemont, "A note on dynamics about the coherent Sun–Earth–Moon collinear libration points," *Astrodynamics Network AstroNet-II*, pp. 183–192, Springer, 2016.

[21] V. Szebehely and E. Grebenikov, "Theory of Orbits-The Restricted Problem of Three Bodies.," *Soviet Astronomy*, Vol. 13, 1969, p. 364.

[22] A. Wintner, "The Analytical Foundation of Celestial Mechanics Princeton Univ," *Press, Princeton, NJ*, 1947.

[23] K. C. Howell, "Families of orbits in the vicinity of the collinear libration points," *The Journal of the Astronautical Sciences*, Vol. 49, No. 1, 2001, pp. 107–125.

[24] D. Grebow, "Generating periodic orbits in the circular restricted three-body problem with applications to lunar south pole coverage," *MSAA Thesis, School of Aeronautics and Astronautics, Purdue University*, 2006, pp. 1–165.

[25] R. Broucke, "Stability of periodic orbits in the elliptic, restricted three-body problem.," *AIAA journal*, Vol. 7, No. 6, 1969, pp. 1003–1009.

[26] K. K. Boudad, K. C. Howell, and D. C. Davis, "Dynamics of synodic resonant near rectilinear halo orbits in the bicircular four-body problem," *Advances in Space Research*, Vol. 66, No. 9, 2020, pp. 2194–2214.

[27] S. Campagnola, M. Lo, and P. Newton, "Subregions of Motion and Elliptic Halo Orbits in the Elliptic Restricted Three-Body Problem," *Proceedings of the 18th AIAA/AAS Space Flight Mechanics Meeting*, 2008, pp. 1541–1556.

[28] E. M. Zimovan-Spreen, K. C. Howell, and D. C. Davis, "Dynamical Structures Nearby NRHOs with Applications to Transfer Design in Cislunar Space," *The Journal of the Astronautical Sciences*, Vol. 69, No. 3, 2022, pp. 718–744.